Available online at www.sciencedirect.com
ScienceDirect
ELSEVIER
Comput. Methods Appl. Mech. Engrg. 196 (2007) 3025–3032
Computer methods in applied mechanics and engineering
www.elsevier.com/locate/cma

The micro-mechanics of cortical shell removal in the human vertebral body

Senthil K. Eswaran [a,b,*], Harun H. Bayraktar [a,b,c], Mark F. Adams [d], Atul Gupta [a,b], Paul F. Hoffmann [a,b], David C. Lee [a], Panayiotis Papadopoulos [b,c], Tony M. Keaveny [a,b,e]

[a] *Orthopaedic Biomechanics Laboratory, 2166 Etcheverry Hall, University of California, Berkeley, CA 94720-1740, USA*
[b] *Department of Mechanical Engineering, University of California, Berkeley, CA 94720, USA*
[c] *Computational Solid Mechanics Laboratory, University of California, Berkeley, CA 94720, USA*
[d] *Department of Applied Physics and Applied Mathematics, Columbia University, New York, NY 10027, USA*
[e] *Department of Bioengineering, University of California, Berkeley, CA 94720, USA*

Received 10 December 2005; received in revised form 10 May 2006; accepted 7 June 2006

Abstract

An improved understanding of the biomechanical role of the vertebral cortical shell with respect to the trabecular bone may improve diagnosis of osteoporosis and provide insight into the effects of disease, aging, and drug treatments. In this study, we present results from finite element simulations of removal of the shell from the vertebral body and the associated mechanical effects in terms of overall change in vertebral structural stiffness and of the tissue-level stresses. Specimen-specific micro-mechanical finite element models of thirteen vertebrae were generated from micro-CT scans with 60-μm voxel size. An algorithm was developed to automatically isolate the thin (and discontinuous) shell and the images were converted into finite element models by mapping each image voxel into a finite element. After removal of the endplates, compressive loading conditions were applied and linear elastic analyses were run for three cases – with and without the shell, and shell-only models. The models contained up to 13.6 million elements and were solved using a maximum of 144 CPUs in parallel, 300 GB memory, and a custom code with a parallel mesh partitioner and algebraic multigrid solver. Results indicated that the shell was on average, 0.38 ± 0.06 mm thick, accounted for 21–39% of the overall bone mass, but accounted for 38–68% of the overall vertebral stiffness. Examination of the tissue-level stresses indicated that this disproportionately large mechanical effect of shell removal was due in part to unloading of the remaining peripheral trabeculae adjacent to the shell. Stress paths were also preferentially within vertically-aligned bone: the cortical shell and vertically-aligned trabeculae. Taken together, these results demonstrate two important roles of the thin vertebral cortical shell: it can carry significant load by virtue of representing a large proportion of the vertically-aligned bone tissue within the vertebra, and, as a shell, it also maximizes the load carrying capacity of the trabecular centrum, particularly around the periphery.

Keywords: Spine biomechanics; Micro-mechanics; Cortical shell; Finite element analysis; Vertebral body; Trabecular bone

1. Introduction

The human lumbar and thoracic vertebrae are major load-bearing bones within the spinal column that consist primarily of highly porous trabecular bone, surrounded by a thin cortical shell. The mechanical integrity of the vertebra is a critical factor in the etiology of age-related osteoporotic fractures and in the support structure for a variety of orthopaedic implants such as pedicle screws and intervertebral disc replacements. An improved understanding of the biomechanical role of the vertebral cortical shell with respect to the trabecular bone may improve diagnosis of osteoporosis and provide insight into the effects of disease,

* Corresponding author. Address: Orthopaedic Biomechanics Laboratory, 2166 Etcheverry Hall, University of California, Berkeley, CA 94720-1740, USA. Tel.: +1 510 642 3787; fax: +1 510 642 6163.
E-mail address: senthilk@me.berkeley.edu (S.K. Eswaran).

0045-7825/$ - see front matter
doi:10.1016/j.cma.2006.06.017

aging, and drug treatments. It may also provide a basis for mechanistic validation of finite element models used for fracture risk prediction [7,11,14,16] and for improved design of spinal implants.

Since the cortical shell is a thin, discontinuous and porous structure, it has been difficult to characterize its mechanical contribution to the overall strength of the vertebral body. While some studies have concluded that the cortical shell takes over 40% of the load [14,23,31], others have concluded that it takes less than 15% [17,26]. The major shortcoming of the experimental studies is controlling the removal process of the shell: if too much is removed, it may induce damage to the trabecular centrum, if too little is removed, the effect of the shell is underestimated. Since the shell is on the order of 0.25–0.4 mm thick [9,22,25,30], it is difficult to remove it in a precise fashion. Continuum-level finite element models [5,7,11,14,16,26] suffer from a simplistic modeling of the shell and its interaction with the trabecular centrum, although these analyses have provided unique insight. For example, it has been shown that the load taken by the shell depends on the location along the superior–inferior axis [5,14,26], as well as the applied boundary conditions [14].

With recent advances in micro-computed tomography (micro-CT) and parallel supercomputer technologies, it is now possible to obtain high-resolution scans of whole bones at a spatial resolution on the order of 50–100 μm and analyze the micro-mechanics of the bones using image-specific finite element analysis at this spatial resolution. Studies using this technique have provided unique insight into the mechanical effects of osteoporosis at the proximal femur [29] and the vertebral body [10,13]. Analyses on the vertebra have shown that the average load fraction taken by the vertebral cortical shell is 0.45 across vertebrae [10], maximum at the mid-section [10,13] and that with osteoporosis, the trabecular micro-structure becomes less resistant to non-habitual loads [13]. Despite these studies, there remains an incomplete understanding of the mechanisms by which the shell contributes to the load-carrying capacity of the vertebra.

As part of an overall effort to understand the micro-mechanics of the human vertebral body, including the specific load sharing role of the cortical shell [10], our goal in this study was to investigate the biomechanical effects of removal of the shell from the vertebral body. Our first objective was to develop an automated technique to digitally identify the geometrically complex cortical shell using micro-CT scans of a series of human vertebral bodies and using this, calculate mean values of shell thickness and the shell's contribution to the total bone mass. Our second objective was to create and analyze three micro-finite element models of each vertebral body: (1) the whole vertebral body; (2) the trabecular centrum alone, having virtually removed the shell from the vertebra; and (3) the isolated cortical shell itself. Data were then analyzed to determine the effects of shell removal and the dependence of these effects, if any, on the density and stiffness of the vertebral body. This study is unique in its precise isolation of the cortical shell and its focus on the micro-mechanics of shell removal.

2. Methods

Thirteen T-10 vertebral bodies obtained from female human cadavers (age range: 54–87 years, 74.6 ± 9.4 years) were scanned at 30-μm voxel size using micro-CT (SCANCO 80, SCANCO Medical AG, Bassersdorf, Switzerland). The voxel size was increased to 60 μm using region averaging to reduce the CPU time required to analyze the resulting finite element models. Next, both superior and inferior cortical endplates were removed from the vertebral body. This was done to facilitate easier application of uniform compressive boundary conditions on the superior and inferior surfaces, a protocol that has also been used in experiments on cadaver vertebrae [19].

A custom program was developed within commercial image processing software (IDL, Research Systems Inc., Boulder, CO) to analyze the morphology of the shell. This program was designed to accomplish three tasks: (1) identify the cortical shell; (2) measure its thickness; and (3) measure its percentage contribution to total bone tissue within the vertebral body. The micro-CT scan data at 60-μm voxel size were analyzed one layer at a time starting at the inferior surface and then proceeding in the superior direction. Each slice of the vertebral body was first divided into four quadrants. Each of these four sections was processed in the same manner. Within each quadrant, the outer edge of the cortical shell was defined as the first filled voxel (i.e., bone tissue) on a line originating from the edge of the image layer (horizontal or vertical depending on the quadrant being processed). The inner edge of the shell was defined as the first empty voxel (i.e., space) after a series of filled voxels along the line. At this point it is important to note that two scenarios can lead to inaccuracies in the cortical shell identification (Fig. 1). The first is the possibility of trabeculae being adjacent to the shell that would artificially increase the thickness of the shell at that location. The second is that the discontinuities in the cortical shell can cause the algorithm to enter the trabecular centrum and count internal trabeculae as part of the shell. Therefore, the program used moving averages and various checks to ensure that these two cases were properly handled during the identification of the cortical shell. The moving average was used to identify sudden increases in shell thickness. Further, if the first filled voxel along the search line was far from the current calculated position of the shell it was ignored. This method allowed us to identify discontinuities in the shell. In order to model the porous nature of the shell, any bone encountered within an average pore size of 180 μm [25] of the outer structure of the shell was identified as part of the shell. The accuracy of our algorithms was verified by visually comparing original scan layers and the identified cortical shell.

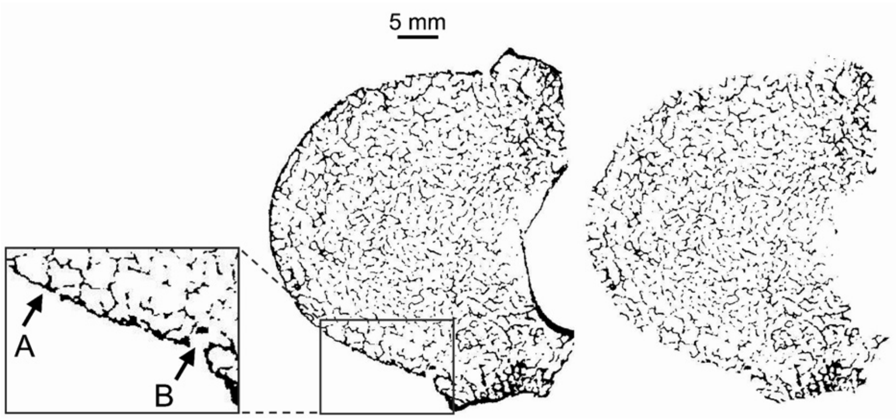

Fig. 1. A transverse image slice of a thresholded vertebral body before (center) and after (right) the shell is removed. The inset on the left shows two important aspects of the shell removal algorithm: (A) trabeculae adjacent to the cortical shell should not be considered as part of the shell and (B) care should be taken to skip discontinuities in the cortical shell and hence avoid identifying trabeculae in the centrum as part of the shell.

The algorithm that calculated the thickness of the cortical shell used the shell image data obtained by the identification program and processed it one layer at a time. The outside and inside edge voxels, and the tangent to the shell edge at the current point were used to obtain the thickness of the shell at each point. The tangent of the shell was obtained by a least squares fit to the position data of shell voxels on both sides of the current point. The thickness of the shell was then calculated as the shortest distance between the outer and inner edges along the line normal to the tangent. The thickness at each point was used to calculate the average thickness of the cortical shell of the vertebral body. The volume of the cortical shell was calculated as the number of filled voxels within the shell image data and shell mass fraction (shell bone mass/total bone mass) was determined.

Three different micro-finite element models were created for each vertebra (Fig. 2): (1) intact vertebral body (intact), (2) trabecular centrum (no-shell), and (3) cortical shell alone (shell-only). These models used 60-μm size 8-node linear hexahedral finite elements with the largest model having around 13.6 million finite elements and 72 million degrees of freedom. All bone tissue was modeled as linear elastic with an elastic modulus of 18.5 GPa and a Poisson's ratio of 0.3. This is reasonable since there is ample evidence that the shell and trabeculae have substantially the same elastic material behavior [20,24,25]. Further, isotropic modeling of the anisotropic bone tissue is also justified since stresses within the trabeculae are mostly along the axes of the trabeculae, and thus along the main principal material orientation. Appropriate frictionless displacement boundary conditions were applied at the superior and inferior surfaces to result in a 1% compression of the vertebral body along the superior–inferior axis. A custom finite element analysis code, which uses parallel mesh partitioning and a state-of-the-art algebraic multigrid iterative solver [1–3], was used for analysis. All models were run on a parallel supercomputer (IBM SP4, IBM Corporation, Armonk, NY) with a maximum of 144 CPUs and 300 GB memory. Due to the use of a highly efficient solver, the analysis of the largest model completed in less than 10 min wall clock time and the total CPU time for the project was just 654 h, corresponding to about 10 h in real time.

The trabecular bone volume fraction for each vertebral body was calculated from a representative volume of trabecular bone, typically a cube 20 mm on a side. The overall structural stiffness of the shell (shell-only model), the

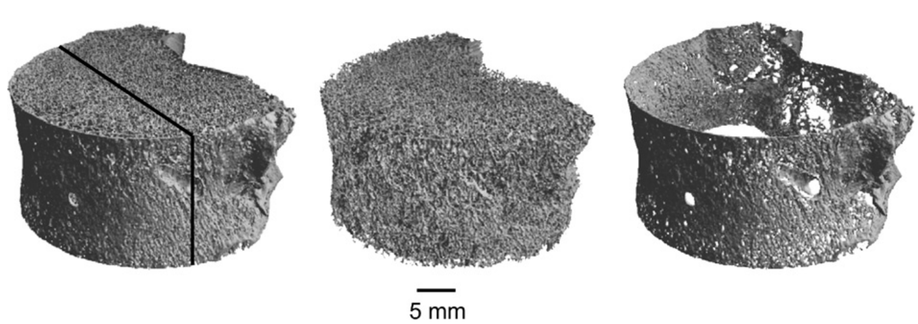

Fig. 2. Renderings of the three micro-finite element models used in this study: intact (left), no-shell (center), and shell-only (right). The location of the mid-frontal slice is shown on the intact model (left). Note that the endplates have been removed for ease of applying boundary conditions on the superior and inferior surfaces that result in 1% compression of the vertebral body.

trabecular bone (no-shell model) and the vertebral body (intact model) were each determined as the ratio of the respective forces generated at the inferior surface of each model to the applied uniform displacement. The influence of the shell removal on the stress distribution within the trabecular bone was analyzed qualitatively using change in von-Mises stress.

3. Results

The average (±SD) thickness of the cortical shell was 0.38 (± 0.06) mm, which is in close agreement with previously reported experimental measurements of the shell thickness [9,22,25,30]. Across all 13 vertebrae, the cortical shell constituted 21–39% (mean ± SD = 0.30 ± 0.05) of the total volume of all bone tissue without including the endplates.

The percent reduction in the overall stiffness of the vertebral body when the shell was virtually removed was substantial, varying from 38% to 68% (mean ± SD = 52 ± 9%; Fig. 3). However, the shell-only model itself had a stiffness of only 2–22% (mean ± SD = 9 ± 6%) of the intact vertebral body. These findings are indicative of a strong interaction between the shell and centrum. The stiffness reduction that occurred with removal of the shell was highly correlated with the shell mass fraction ($R^2 = 0.93$, $p < 0.0001$, Fig. 4b) but was only weakly correlated with the volume fraction of the trabecular region of interest within the centrum ($R^2 = 0.42$, $p < 0.02$, Fig. 4a) and was not correlated ($p = 0.72$) with the original stiffness of the vertebra.

Examination of the tissue-level stress distributions within the vertebral body demonstrated that the structural effects of cortical shell removal were due to both loss of the shell itself, and unloading of the peripheral trabecular bone. Trabeculae aligned in the loading direction as well as the cortical shell – i.e., the vertically-aligned bone material – were the primary load carrying components (Fig. 5). Further, the removal of the shell caused substantial unloading of peripheral trabeculae adjacent to the shell and the distribution of unloaded trabeculae was heterogeneous across transverse slices of the vertebral body (Fig. 5). In particular, the region of unloading was typically smaller at the mid-transverse section compared to transverse sections near the ends of the vertebra.

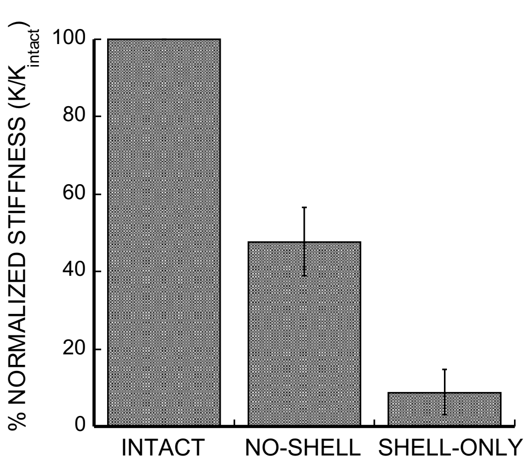

Fig. 3. Normalized stiffness of the three models (stiffness divided by intact stiffness, expressed as a percentage). Data show mean values ± SD for $n = 13$ vertebrae. While the stiffness of the shell alone was only 9% of the intact vertebral body stiffness on average, the reduction in the vertebral body stiffness due to shell removal was 52% on average across the 13 vertebrae.

4. Discussion

This study was performed in the context of an overall effort to improve understanding of the micro-mechanics of the human vertebral body. Towards that end, we developed a method to automatically isolate the cortical shell in micro-CT scans of a vertebral body. Coupling of this technique with large-scale finite element analyses allowed us to study the micro-mechanics associated with removal of the cortical shell from the vertebral body. Our results showed that the thin cortical shell, which accounted for 30% of the bone tissue on average, contributed 52% of the overall stiffness – a disproportional role with respect to its bone mass. The very low stiffness of the shell alone demonstrated that without the trabecular centrum, the shell has little structural integrity (as would be expected for any "shell"). Analysis of the tissue-level stress distributions demonstrated that the highest stressed regions were invariably those within vertically-aligned bone tissue, be it the cortical shell or vertically-oriented trabeculae. Further, the peripheral trabeculae became substantially unloaded when the shell was removed due to the loss of connectivity with the shell, particularly towards the ends of the vertebra. Taken together, these findings demonstrate two important roles of the vertebral cortical shell: it can carry significant load by virtue of representing a large proportion of the vertically-aligned bone tissue within the vertebra, and, as a shell, it also maximizes the load carrying capacity of the trabecular centrum, particularly with the trabeculae around the periphery. As such, these results give significant new insight into the micro-mechanics of the effects of shell removal, and in turn, of the vertebral body.

The main strength of this study was the use of high-resolution micro-CT image data processing to create virtual models of the cortical shell, trabecular centrum, and the intact vertebral body and application of this technique to a series of vertebral bodies. This allowed us to determine the mechanical properties and tissue-level stress distributions for the same vertebral body after the removal of the shell, which is impossible experimentally. The multiscale analysis enabled us to independently study the micro- and macro-mechanics of each component and provided detailed information regarding the interaction between the cortical shell and trabecular centrum. Such mechanical interactions may not be captured using continuum-level finite element models [7,11,14,16] because in these models, the peripheral trabecular bone's load bearing capacity is

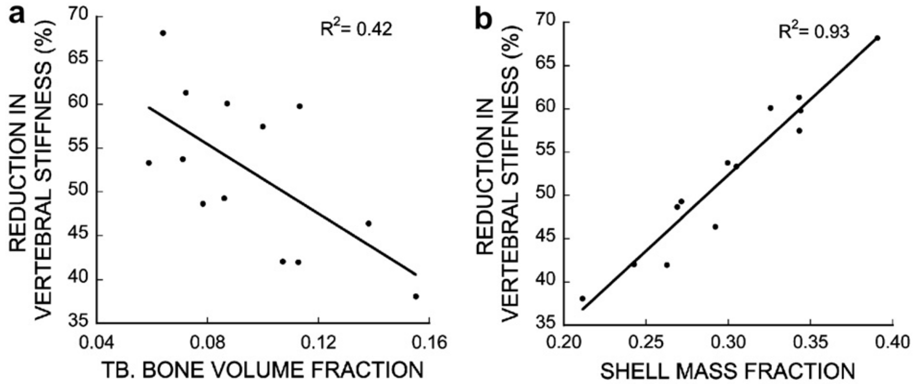

Fig. 4. Variation of the percent reduction in vertebral stiffness due to shell removal with (a) trabecular bone volume fraction and (b) shell mass fraction.

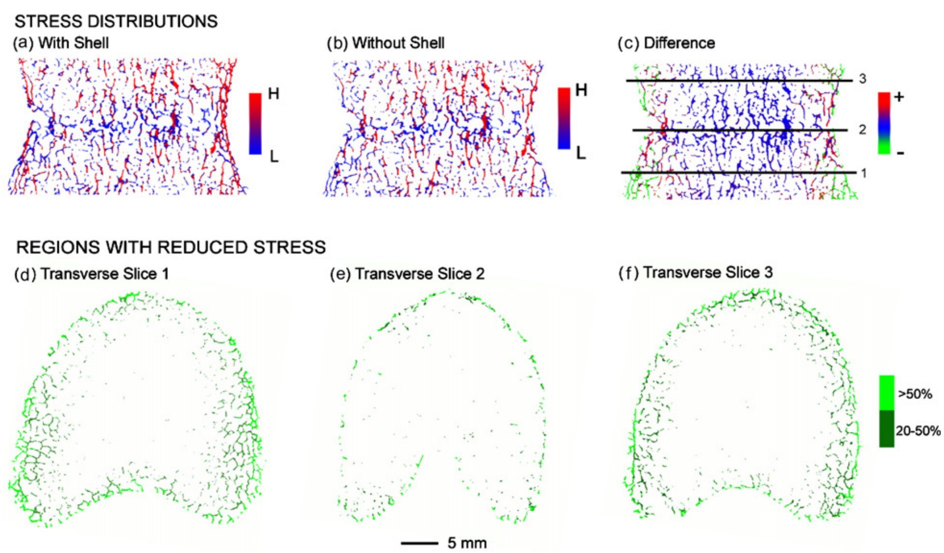

Fig. 5. Distribution of tissue-level von-Mises stresses in a mid-frontal cross-section (see Fig. 2 for location of mid-frontal slice) for a typical specimen. Both intact (a) and no-shell (b) models are shown. Differences in von Mises stresses upon removal of the shell are also shown (c). The distribution of unloaded trabeculae (greater than 20% reduction) in three transverse slices (d, e, f) shows the heterogeneity in the unloading region across the vertebral body. In particular, the region of unloading at the mid-transverse cross-section was typically smaller compared to cross-sections near the ends of the vertebra. Key: H: high; L: low; + and − indicate that stresses increased or decreased with shell removal, respectively.

not contingent on the presence of the cortical bone whereas in the micro-mechanical models – and the real bone – it is. Our algorithms that were developed to identify and remove the cortical shell were verified visually. Further evidence of the accuracy of these algorithms was the fact that the cortical shell thickness obtained in this study fell within the ranges reported by previous experimental studies [9,22,25,30]. Our application of these techniques to multiple vertebral bodies enabled us to apply a statistical approach to analysis of our data, simulating variable responses associated with the different vertebrae, as would be encountered in a real experiment.

The main caveat of this study lies in the removal of the endplates for the finite element analyses. As has been done previously in experimental studies [19], the endplates were removed to simplify application of the boundary conditions and avoid uncertainties associated with the disc properties and variations in endplate morphology that occurs across specimens. As a result of these boundary conditions, the absolute quantitative effects reported here would likely differ from what would occur if the endplates had been left intact, but the effect may not be substantial for a global metric such as stiffness reduction due to shell removal. For example, even in our analysis of load sharing between the cortical and trabecular bone of these same vertebrae [10] which calculated load fractions locally at each cross-section, we found that the average load fraction taken by the cortical shell at mid-section was 0.45 with endplates compared to 0.52 without endplates. The effects of loading through an intervertebral disc were not included in our analyses, and such loading may well alter stress transfer through the vertebra [26]. However, because each specimen served as its own control in computing the effects of shell removal, these limitations should be mostly mitigated as regards to the general effects reported, i.e., the disproportional role of the shell compared to its mass, stress transfer through vertically-orientated bone tissue, and the unloading of peripheral trabeculae upon shell removal. A second and related limitation is that we only addressed the response to compressive-type loads, and even for this case, the loads were applied in a uniform manner without the presence of the endplates. It is expected that stress distributions will differ for different load cases, although we expect the strong interaction between the shell and the centrum to persist and perhaps even to be accentuated for bending type loading, for which the peripheral bone plays a more important role [8]. Another possible limitation is that bone tissue was modeled as a homogenous material, not taking into account any spatial variation in tissue elastic properties due to different levels of mineralization. Results of previous finite element studies [15,28] suggest that the effects of such variations will likely not affect the load transfer mechanisms between the trabecular centrum and cortical shell. Finally, our linear elastic finite element analysis does not capture non-linearities that may be important in the failure behavior of the vertebral body such as localized large deformation effects [4,18,21,27] and material failure at the tissue-level (e.g., micro-damage). However, this study only aimed at studying the micro-mechanics of the vertebral body under daily (i.e., normal) loads that are unlikely to cause failure and our focus was on effect of shell removal during such elastic behavior. Even so, the observed reduction in vertebral stiffness for one specimen obtained from linear analysis (44%) compared well with the reduction in the load-carrying capacity of the vertebral body computed in a preliminary fully-nonlinear analysis (47–49%) [12]. Taken together with previous studies which have reported highly significant correlations between finite element predictions of vertebral stiffness and experimental measures of vertebral strength [7], the trends seen here for changes in stiffness are expected to be indicative of changes in strength. Moreover, since loss of connectivity with the surrounding cortical shell is the underlying mechanism causing the unloading of the peripheral trabeculae during shell removal, it is unlikely that our conclusion regarding substantial unloading of the peripheral trabeculae would be affected by incorporating failure behavior of the vertebral body.

Realizing the potential effect of endplate removal on the absolute effects reported here, our results are consistent with most of the available experimental data on the topic of biomechanical effects of shell removal for the human vertebra. The range of reduction (38–68%) reported here for vertebral stiffness due to virtual removal of the shell compares well with other experimental studies in which the shell was physically removed: a 45–75% reduction in vertebral strength observed by Rockoff et al. [23] and a 40% mean strength reduction reported by Yoganandan et al. [31]. Since we have shown that a ring of peripheral trabecular bone is substantially unloaded due to shell removal (Fig. 5), any possible damage to this bone during (real) shell removal would not result in appreciable reductions in strength beyond that due to loss of the shell. We suggest then that the low value of strength reduction (10%) reported by Mcbroom et al. [17] is possibly a result of their concern not to damage the underlying trabecular bone – that in fact they did not remove all the shell by their careful manual sanding process. Taken together, the weight of the available evidence clearly indicates that removal of the shell results in substantial reductions in the load carrying capacity of the vertebral body. Our results are unique in that they provide a mechanistic understanding of such effects.

Our results also provide insight into interpretation of results from clinical-resolution (1–2 mm sized finite elements) finite element models that are generated from quantitative computed tomography (QCT) scans of either cadaver or live subject bones and that also virtually removed the shell. Faulkner et al. [11] used 3–5 mm sized elements and concluded that the contribution of the shell to vertebral strength was higher in osteoporotic vertebra. Though the value of strength reduction of normal bones (10%) reported in their study was much lower (possibly due to discretization effects since their element sizes were so large), their result is consistent with our finding from the shell removal analyses that the reduction in the vertebral stiffness is greater in low-density vertebra (Fig. 4a). Crawford et al. [6], using 1 mm sized elements, reached a similar conclusion that the peripheral bone (1–3 mm outer layers, including the cortical shell) plays a substantial role in the vertebral strength in their cohort of elderly women, the effect being greater in weaker bones. In effect, one can interpret removal of the 1–3 mm of outer bone in the clinical resolution models as being equivalent to removal of the cortical shell, since our analyses show that real removal of the shell should be accompanied by substantial unloading of the adjacent trabeculae, particularly towards the ends of the vertebra. The consistency of the results from this micro-mechanical study with clinical QCT-based studies despite the overestimation of the shell thickness in clinical QCT images [25] is likely because the QCT density variations across the 1 mm elements effectively capture the underlying increased bone mass associated with the shell. Thus, our micro-mechanical analyses provide a level of validation of these clinical resolution parameter studies – or at least offer an interpretation of what those models simulate when they remove the outer bone. One general implication of this finding is that it may not be necessary to explicitly capture the shell in the finite element models in order to compute its structural effects.

The results from this study provide unique insight into mechanisms of load transmission within a vertebral body. A first mechanism is the interaction of the peripheral trabeculae and the cortical shell. The cortical shell provides a load path for the peripheral trabecular bone, which, in the absence of the shell, would be unloaded because of the disconnected nature of the trabeculae at the edge (Fig. 5). Similarly, the peripheral trabecular bone enables the cortical shell to carry load, evident from our results that the shell alone cannot carry much load due to its discontinuous, thin, and curved nature. A second mechanism is that it is primarily the vertically-aligned bone tissue within the vertebra that supports the axial load. Therefore, the sharing of axial compressive load between the shell and the centrum involves primarily the vertical trabeculae of the centrum. Horizontal trabeculae only contribute indirectly to supporting the axial load. And since the cortical shell represents a sizable proportion of the vertically-aligned bone tissue within the vertebra, it too carries significant levels of load. With the hindsight provided by this study, it is understandable why measures of vertebral trabecular density taken from the mid-centrum, even when coupled with measures of vertebral geometry, are not such sensitive predictors of whole vertebral strength [7].

Acknowledgements

Funding was provided by National Institutes of Health grant AR049828 and Department of Energy grants DE-FG03-94ER25219 and DE-FG03-94ER25206. Supercomputer resources were available through grant UCB-254 from the National Partnership for Computational Infrastructure. Human tissue was obtained from National Disease Research Interchange and University of California at San Francisco. All micro-CT imaging was performed at Exponent, Inc. (Philadelphia, PA). Thanks to Dr. Dan Mazzucco and Jennifer Vondran for imaging the specimens, Bethany Baumbach for editorial assistance and Eric Wong for technical assistance. Dr. Keaveny has a financial interest in O.N. Diagnostics and both he and the company may benefit from the results of this research.

References

[1] M. Adams, Evaluation of three unstructured multigrid methods on 3D finite element problems in solid mechanics, Int. J. Numer. Meth. Engrg. 44 (2002) 519–534.

[2] M.F. Adams, H.H. Bayraktar, T.M. Keaveny, P. Papadopoulos, Applications of algebraic multigrid to large-scale finite element analysis of whole bone micro-mechanics on the IBM SP, in: ACM/IEEE Supercomputing, Phoenix, AZ, 2003.

[3] M.F. Adams, H.H. Bayraktar, T.M. Keaveny, P. Papadopoulos, Ultrascalable implicit finite element analyses in solid mechanics with over a half a billion degrees of freedom, in: ACM/IEEE Proceedings of SC2004: High Performance Networking and Computing, 2004.

[4] G. Bevill, S.K. Eswaran, A. Gupta, P. Papadopoulos, T.M. Keaveny, Influence of bone volume fraction and architecture on computed large-deformation failure mechanisms in human trabecular bone, Bone 39 (2006) 1218–1225.

[5] K.D. Cao, M.J. Grimm, K.H. Yang, Load sharing within a human lumbar vertebral body using finite element method, Spine 26 (2001) 253–260.

[6] P. Crawford, J.J. Camp, S. Khosla, T.M. Keaveny, Structure-function relationships and determinants of vertebral strength in elderly women, Trans. Orthop. Res. Soc., Washington, DC, 2005, p. 0032.

[7] R.P. Crawford, C.E. Cann, T.M. Keaveny, Finite element models predict in vitro vertebral body compressive strength better than quantitative computed tomography, Bone 33 (2003) 744–750.

[8] R.P. Crawford, T.M. Keaveny, Relationship between axial and bending behaviors of the human thoracolumbar vertebra, Spine 29 (2004) 2248–2255.

[9] W.T. Edwards, Y.G. Zheng, L.A. Ferrara, H.A. Yuan, Structural features and thickness of the vertebral cortex in the thoracolumbar spine, Spine 26 (2001) 218–225.

[10] S.K. Eswaran, A. Gupta, M.F. Adams, T.M. Keaveny, Cortical and trabecular load sharing in the human vertebral body, J. Bone Miner. Res. 21 (2006) 307–314.

[11] K.G. Faulkner, C.E. Cann, B.H. Hasegawa, Effect of bone distribution on vertebral strength: assessment with patient-specific nonlinear finite element analysis, Radiology 179 (1991) 669–674.

[12] A. Gupta, M.F. Adams, S.K. Eswaran, T.M. Keaveny, Nonlinear finite element analysis of human bone, US National Congress on Computational Mechanics, Austin, TX, 2005.

[13] J. Homminga, B. Van-Rietbergen, E.M. Lochmuller, H. Weinans, F. Eckstein, R. Huiskes, The osteoporotic vertebral structure is well adapted to the loads of daily life, but not to infrequent error loads, Bone 34 (2004) 510–516.

[14] J. Homminga, H. Weinans, W. Gowin, D. Felsenberg, R. Huiskes, Osteoporosis changes the amount of vertebral trabecular bone at risk of fracture but not the vertebral load distribution, Spine 26 (2001) 1555–1561.

[15] M.J. Jaasma, H.H. Bayraktar, G.L. Niebur, T.M. Keaveny, Biomechanical effects of intraspecimen variations in tissue modulus for trabecular bone, J. Biomech. 35 (2002) 237–246.

[16] M.A. Liebschner, D.L. Kopperdahl, W.S. Rosenberg, T.M. Keaveny, Finite element modeling of the human thoracolumbar spine, Spine 28 (2003) 559–565.

[17] R.J. McBroom, W.C. Hayes, W.T. Edwards, R.P. Goldberg, A.A. White, Prediction of vertebral body compressive fracture using quantitative computed-tomography, J. Bone Joint Surg. – Am. Volume 67A (1985) 1206–1214.

[18] E.F. Morgan, H.H. Bayraktar, O.C. Yeh, S. Majumdar, A. Burghardt, T.M. Keaveny, Contribution of inter-site variations in architecture to trabecular bone apparent yield strains, J. Biomech. 37 (2004) 1413–1420.

[19] L. Mosekilde, S.M. Bentzen, G. Ortoft, J. Jorgensen, The predictive value of quantitative computed-tomography for vertebral body compressive strength and ash density, Bone 10 (1989) 465–470.

[20] L. Mosekilde, Vertebral structure and strength in-vivo and in-vitro, Calcif. Tissue Int. 53 (1993) S121–S126.

[21] R. Muller, S.C. Gerber, W.C. Hayes, Micro-compression: a novel technique for the nondestructive assessment of local bone failure, Technol. Health Care 6 (1998) 433–444.

[22] H. Ritzel, M. Amling, M. Pösl, M. Hahn, G. Delling, The thickness of human vertebral cortical bone and its changes in aging and osteoporosis: a histomorphometric analysis of the complete spinal column from thirty-seven autopsy specimens, J. Bone Miner. Res. 12 (1997) 89–95.

[23] S.D. Rockoff, E. Sweet, J. Bleustein, The relative contribution of trabecular and cortical bone to the strength of human lumbar vertebrae, Calcif. Tissue Res. 3 (1969) 163–175.

[24] M.E. Roy, J.Y. Rho, T.Y. Tsui, N.D. Evans, G.M. Pharr, Mechanical and morphological variation of the human lumbar vertebral cortical and trabecular bone, J. Biomed. Mater. Res. 44 (1999) 191–197.

[25] M.J. Silva, C. Wang, T.M. Keaveny, W.C. Hayes, Direct and computed tomography thickness measurements of the human lumbar vertebral shell and endplate, Bone 15 (1994) 409–414.

[26] M.J. Silva, T.M. Keaveny, W.C. Hayes, Load sharing between the shell and centrum in the lumbar vertebral body, Spine 22 (1997) 140–150.

[27] J.S. Stolken, J.H. Kinney, On the importance of geometric nonlinearity in finite-element simulations of trabecular bone failure, Bone 33 (2003) 494–504.

[28] J.C. van der Linden, D.H. Birkenhager-Frenkel, J.A. Verhaar, H. Weinans, Trabecular bone's mechanical properties are affected by its non-uniform mineral distribution, J. Biomech. 34 (2001) 1573–1580.

[29] B. Van Rietbergen, R. Huiskes, F. Eckstein, P. Ruegsegger, Trabecular bone tissue strains in the healthy and osteoporotic human femur, J. Bone Miner. Res. 18 (2003) 1781–1788.
[30] A. Vesterby, L. Mosekilde, H.J.G. Gundersen, F. Melsen, L. Mosekilde, K. Holem, S. Sorensen, Biologically meaningful determinants of the in vitro strength of lumbar vertebrae, Bone 12 (1991) 219–224.
[31] N. Yoganandan, J.B. Myklebust, J.F. Cusick, C.R. Wilson, A. Sances, Functional biomechanics of the thoracolumbar vertebral cortex, Clin. Biomech. 3 (1988) 11–18.